

## EXPERIMENTAL AND MATHEMATICAL MODEL FOR EVALUATION OF LDL UPTAKE BY THE ISOLATED BLOOD VESSELS

Maja Colic<sup>1</sup>, Vuk Jokovic<sup>2</sup>

<sup>1</sup>Department of Physiology, Medical Faculty, University of Kragujevac, Serbia

<sup>2</sup>Department of Vascular Surgery, Clinical Center, Kragujevac, Serbia

## EKSPERIMENTALNI I MATEMATIČKI MODEL ZA PROCENU TRANSPORTA LDL-A U IZOLOVANI KRVNI SUD

Maja Čolić<sup>1</sup>, Vuk Joković<sup>2</sup>

<sup>1</sup>Institut za fiziologiju, Medicinski fakultet, Univerzitet u Kragujevcu, Kragujevac

<sup>2</sup>Centar za vaskularnu hirurgiju, Klinički centar „Kragujevac“, Kragujevac

### ABSTRACT

**Objective.** The aim of this study is to present the experimental model which can be used to determine LDL transport into the blood vessel wall.

**Method.** We used isolated rabbit carotid arteries under physiologically relevant constant pressure and perfusion flow in conditions more similar to *in vivo*. We used Rapid dual-isotope dilution method, Steady - state method, testing of transport of LDL-before and after removal of the endothelium, in conditions with intact endothelium and after its removal.

**Results.** First we used Rapid dual-isotope dilution method and the data obtained showed that the transport of LDL could not be precisely determined in this way because it was in the range of standard error. Then we used Steady - state method and uptake ( $U_s$ ) was  $3.52 \pm 1.07\%$  at higher pressure ( $140 \pm 10$  mmHg) than at lower pressure ( $p < 0.05$ ). Also, LDL uptake was evaluated before and after the endothelium removal. The results after endothelial removal showed that  $U_s$  of LDL was almost 3 times higher (9.2%) than with intact endothelium ( $p < 0.05$ ) and that the accumulation of LDL in the blood vessel wall was 0.1% (0.06% in intact endothelium) indicating that intact endothelium was a strong barrier.

**Conclusion.** Our experimental model and applied mathematical procedures can provide a precise description of the LDL uptake by the blood vessel wall.

**Key words:** lipoproteins, LDL; blood vessels; endothelium; biological transport; radioactive tracers.

### SAŽETAK

**Cilj.** Cilj ove studije bio je da predstavi eksperimentalni model kojim se može utvrditi transport LDL-a u zid krvnog suda.

**Metod.** Izolovane karotidne arterije zečeva tretirali smo u uslovima fizioloških vrednosti pritiska i pri perfuzionom protoku koji je najbliži *in vivo* uslovima. Korišćeni su „Rapid dual-isotope“ dilucioni metod, „Steady-state“ metod, ispitivanje transporta LDL-a pre i posle uklanjanja endotela, u uslovima intaktnog i posle uklanjanja endotela.

**Rezultati.** Prvo smo koristili „Rapid dual-isotope“ dilucioni metod i dobijeni podaci pokazali su da se transport LDL-a ne može na ovaj način precizno utvrditi, jer je u granicama standardne greške. Zatim smo koristili „Steady-state“ metod i na višem pritisku ( $140 \pm 10$  mmHg) preuzimanje LDL-a je bilo  $3,52 \pm 1,07\%$  u odnosu na niži pritisak ( $p < 0,05$ ). Takođe smo ispitivali transport LDL-a pre i posle uklanjanja endotela. U uslovima posle uklanjanja endotela rezultati su pokazali da je preuzeto skoro 3 puta više LDL-a (9,2%) u odnosu na intaktni endotel ( $p < 0,05$ ) i da je nakupljanje LDL-a u zidu krvnog suda bilo 0,1% (dok je u intaktnom endotelu bilo 0,06%) što ukazuje na to da je intaktni endotel snažna barijera.

**Zaključak.** Dobijeni rezultati ukazuju na to da primenjen eksperimentalni i matematički model predstavlja preciznu metodu za procenu preuzimanja LDL-a od strane zida krvnog suda.

**Gljučne reči:** lipoproteini, LDL; krvni sudovi; endotelijum; biološki transport; radioaktivni obeleživači.

### INTRODUCTION

Atherosclerosis represents a large-arteries disease in which lipoproteins are accumulated within the arterial wall (1, 2). Atherogenic molecules, such as low-density lipoprotein (LDL) play an important role in the development of atherosclerosis (3). Except LDL, which is the crucial factor for atherosclerosis, many other parameters have also been established as important. These include wall thickness, wall composition, transmural pressure etc., however, it has not been clearly determined

which of them has the highest impact (3-8). Increased permeability of LDL in endothelium has been reported in some earlier research studies done on hypertensive animals (9, 10). There are some indications that hypertension enhances LDL entry into the intima by changing the permeability of the endothelium (9, 10). Previous *in vitro* studies indicated that stretching of the arterial wall induced by pressure is the major factor of LDL accumulation in atherosclerotic disease and the other mass transport into the arterial wall, especially in the inner section of the vessel (4, 11, 12). It has also been suggested

that LDL transendothelial transport is predominantly determined by the leaky junctions pathway. All previous studies which aimed to explain the mechanisms of LDL transport and accumulation in the blood vessel wall were performed either on isolated blood vessel segments without dynamic flow and shear-stress conditions (11, 13, 14) or *in vitro* using cultured endothelial cell mono-layers (4) or they were performed by using mathematical and computational models of blood vessels (3, 15, 16). Keeping all this in mind, we researched the LDL uptake (transport) into the blood vessel wall, under physiologically relevant constant pressure and perfusion flow (more similar to *in vivo* conditions), in the isolated rabbit carotid artery. Moreover, what we wanted to evaluate was a new method which could be used to determine LDL transport into blood vessel wall.

## MATERIAL AND METHODS

*Ex vivo* blood vessels experiments were performed on the isolated rabbit left and right common carotid artery. All experiments were performed in accordance with the Animals Scientific Procedures Act 1986 (UK) and Local Ethical Guidelines.

### 2.1. Blood vessel preparation

New Zealand White rabbits of both sexes ( $n=5$ ) weighing 3.5-4 kg were anesthetized by using sodium pentobarbital (0.5 mg/kg of body weight, *i.v.*) and ketamine (0.5 mg/kg of body weight) (Laboratory Sanderson, Santiago, Chile) (17). Blood vessel was excised and placed in the water bath. Cannulas with equally matched tip diameters (2 mm) were mounted at proximal (cardiac) and distal (cranial) ends of the blood vessel and the lumen was perfused with Krebs-Ringer physiological solution (KRS), using the peristaltic pump at 1 mL/min. The perfusate was continuously bubbled with a 95% O<sub>2</sub> and 5% CO<sub>2</sub>, with the pH adjusted to 7.4 at 37°C. The blood vessel was stretched to its approximate *in vivo* length. The distal cannula was connected to the resistance changing device and perfusion pressure was measured by using pressure transducer. The blood vessel was considered viable if it contracted when 25 mM KCl was added to the bath, as well as if the presence of functional endothelium was verified by dilation with Ach (1  $\mu$ M) at the end of experiment.

### 2.2. Rapid dual –isotope dilution method

This method measures the relative extraction (uptake) of the test molecule (<sup>125</sup>I-LDL) in relation to an extracellular referent tracer (<sup>99m</sup>Tc-Nanocis, EBD) as it transits through the blood vessel (18, 19). Transport parameters obtained from the rapid dual isotope dilution

technique allow calculation of dynamics and understanding the mechanism of test molecule transport from intravascular space to the blood vessel wall. Before the investigation of molecule uptake test, the series of technical (control) experiments had been performed in order to allow standardization of the experimental protocol.

#### 2.2.1 Experimental protocol, Dilution profiles (Evans Blue Dye, <sup>99m</sup>Tc-Nanocis)

Following temperature equilibration (37°C) with physiological buffer, perfusion flow of 1 mL min<sup>-1</sup>, a 100  $\mu$ L bolus was injected into the perfusion system containing referent tracer (Evans Blue Dye solution -EBD solution, <sup>99m</sup>Tc-Nanocis). The first 15 samples (3 drops in each sample) and 9 cumulative 3 min samples of perfusion effluent were sequentially collected. The first 15 samples were prepared for measurement of tracer concentration by adding physiological buffer until the final volume of 3 mL/sample. Tracer concentration in the cumulative samples was estimated without dilution. EBD concentration in each sample, as well as in the three standard EBD solutions, was estimated by measuring the absorbance value (Micro-sample spectrophotometer, Gilford Instrument). The absorbance intensity is proportional to EBD concentration which is used to obtain perfusion concentration-time curves, *i.e.* dilution profiles for Evans Blue Dye. Measurements of perfusion effluent samples containing <sup>99m</sup>Tc-Nanocis were performed by means of gamma counter (Wallac Wizard 1400). The radioactivity of isotope in the perfusion effluent samples (as a percentage of the injected dose) was plotted against the collection time, in order to obtain radioactivity-time curves, *i.e.* dilution profiles for the investigated molecule.

All control experiments were performed by using the plastic tube instead of the blood vessel under the experimental conditions: constant flow of 1, 2, 3 mL/min.; perfusion pressure of 100, 130, 160, 190 mmHg; medium temperature of 37°C). We have performed the following activities using the plastic tube instead of the blood vessel to determine:

- The correction factors for the dilution profiles of potential referent tracers (EBD, <sup>99m</sup>Tc-Nanocis);
- The optimal radioactivity for the test tracers (<sup>125</sup>I-LDL) in the infusion bolus that is sufficient to produce detectable dilution profiles.

#### 2.2.2 Mathematical analysis of dilution profiles

Experimentally obtained dilution profiles for EBD and <sup>99m</sup>Tc-Nanocis are presented in Figure 1. In this figure we present the fitted values of experimentally obtained data. Both curves were fitted ( $R^2 \geq 0.98$ ) by means of the following equation:

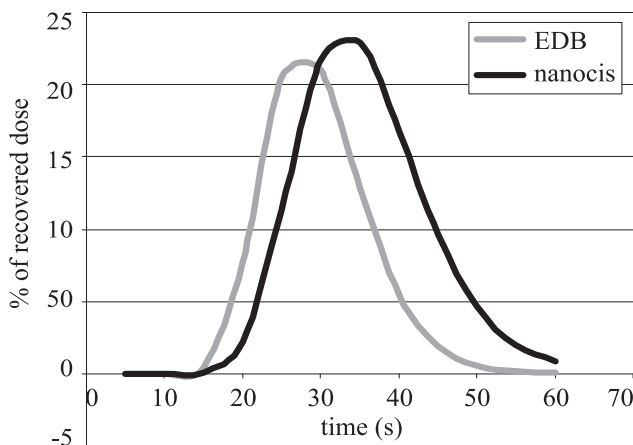


Figure 1. Dilution profiles of EBD and <sup>99m</sup>Tc-Nanocis.

$$y = ae^{-\left[-0.5 \left( \frac{\ln\left(\frac{x}{x_0}\right)}{b} \right)^2\right]} \quad (\text{Eq. 1})$$

where y is percent of recovered dose, and x is time (in seconds).

It is obvious from the Figure 1 that the maximal recovered doses of EBD and <sup>99m</sup>Tc-Nanocis do not appear at the same time indicating different convective diffusion properties of those two molecules. Thus, direct mathematical evaluation of the test tracer uptake could not be possible without the correction of dilution profiles for that difference. By dividing EBD dilution profile by <sup>99m</sup>Tc-Nanocis dilution profile corresponding values, we obtained corrective factors by which <sup>99m</sup>Tc-Nanocis dilution profile has to be multiplied (for each time period) to achieve the full overlap of those dilution profiles. This overlap is supposed to occur due to both traces' injection into the plastic tube (instead of the blood vessel), so the full recovery in each time interval is positively supposed (no uptake for both tracers). In that way, <sup>99m</sup>Tc-Nanocis can be used as a referent tracer; no matter if convective diffusion difference does exist.

Even EBD dilution profiles obtained from the experiments performed in the plastic tube show almost full overlap with <sup>125</sup>I-LDL dilution profiles, the <sup>99m</sup>Tc-Nanocis was used as referent tracer in further investigations, because EBD can pass the endothelial barrier if it is not absolutely intact.

### 2.2.3 <sup>125</sup>I-LDL (test tracer) and <sup>99m</sup>Tc-Nanocis (referent tracer) dilution profiles in the isolated blood vessels.

Rapid dual-isotope dilution method for <sup>125</sup>I-LDL (test tracer) and <sup>99m</sup>Tc-Nanocis (referent tracer) was performed as described above (Section 2.2). Measurements of perfusion effluent samples containing <sup>125</sup>I-LDL were performed by means of the gamma counter (Wallac Wizard 1400). The <sup>125</sup>I-LDL uptake (Us %) is derived from the difference between the <sup>99m</sup>Tc-Nanocis value and that of <sup>125</sup>I-LDL recovery in each sample.

## 2.3. Steady state method

The isolated blood vessel was placed into the water bath with physiological buffer. After the equilibration period (20-30 min) at constant perfusion flow of 1 mL/min Resistance changing device was applied to achieve a constant perfusion pressure (70 ± 10 and 140 ± 10 mmHg). When target pressure was achieved, the period of equilibration (15-30 min) was allowed. Then, the <sup>125</sup>I-LDL standard solution (100 µL/min) was continuously injected into the blood vessel (inflow dose), using rapid infusion pump for 10 minutes. Automatic sampler that allows precise and automatic collection of samples was used to continuously collect the first 12 samples (cumulative 1 min samples of perfusion effluent) and 6 cumulative 3 min samples. The radioactivity in each sample represents the outflow dose in corresponding time period. The first 12 samples were prepared for measurement of <sup>125</sup>I-LDL specific activity by adding physiological buffer until the final volume of 3 mL/sample. <sup>125</sup>I-LDL specific activity in the 3 min cumulative samples was estimated without <sup>125</sup>I-LDL dilution.

After sampling, the blood vessel was cut onto 3 segments (proximal – cardiac, medial and distal – cranial) and the radioactivity accumulation of the <sup>125</sup>I-LDL in the wall was measured in each segment with gamma counter (Wallac Wizard 1400).

### 2.3.1 <sup>125</sup>I-LDL dilution profiles

<sup>125</sup>I-LDL specific activity in each sample was measured with gamma counter (Wallac Wizard 1400). <sup>125</sup>I-LDL specific activity in each sample was used to obtain radioactivity - time curves, i.e. dilution profiles for <sup>125</sup>I-LDL during its flow through blood vessel at constant perfusion pressure. <sup>125</sup>I-LDL specific activity in the first 10 samples during the inflow period was used for the creation of the dilution profile curve (figure 2 and 4). The <sup>125</sup>I-LDL specific activity in the 11th and 12th sample as well as in the next 6 of 3 min cumulative samples was used to create the dilution profile curve for the radioactivity recovery in the washout period (Figure 2).

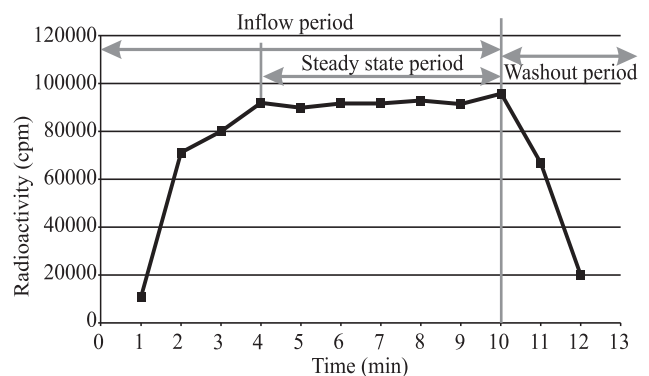


Figure 2. Experimentally obtained dilution profile curve (outflow doses in first 12 samples).

### 2.3.2 Mathematical analyses of dilution profiles

Experimentally obtained dilution profile curves within the inflow period were fitted by using the following exponential equation (20):

$$y = a(1 - e^{-bx}) \quad (\text{Eq. 2})$$

where  $y$  is the specific radioactivity (cpm) and  $x$  has time units (min). Also,  $a$  and  $b$  are the coefficients of this relation and  $a$  has radioactivity units (cpm) and  $b$  has time units (1/min).

This function is shown in Figure 3 as the radioactivity vs. time curve. The constant  $a$  represents the maximum developed radioactivity, i.e. the radioactivity corresponding to the steady state period.

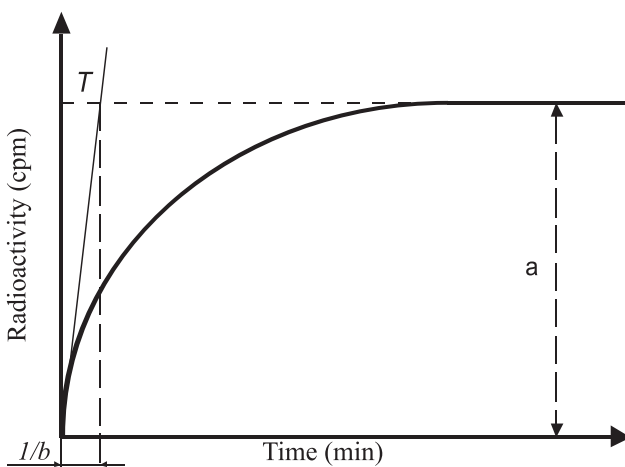


Figure 3. The radioactivity-time relation.

We introduce a dominant time constant ( $T$ ) as the time value corresponding to the cross section point between the asymptote of the exponential curve and the tangent of the exponential curve at the zero point. This constant follows from the function:  $T = 1/b$

We consider that the alternate steady state is reached for  $t = 5T$  ( $t = \text{time}$ ), because in this case  $e^{-t/T} = e^{-5} \approx 0$ , and  $y \approx a$ .

Experimentally obtained dilution profile curves within the washout period were fitted by using the following exponential equation:

$$y = ae^{-bx} \quad (\text{Eq. 3})$$

where  $y$  is the specific radioactivity (cpm) and  $x$  is the time (minutes). Also,  $a$  and  $b$  are the coefficients of this relation. The coefficient  $a$  is the same in the Eq. 3 and Eq. 2.

We consider that the radioactivity values approaches the zero for  $-bx = -5$ , because in this case  $e^{-bx} = e^{-5} \approx 0$ , and  $y \approx 0$ .

Experimentally obtained dilution profile curve within the inflow period fitted using Eq. 2 is shown in Figure 4.

The steady state uptake was calculated as a difference between the inflow dose of  $^{125}\text{I}$ -LDL and the outflow dose (in samples) within the period of the steady state.

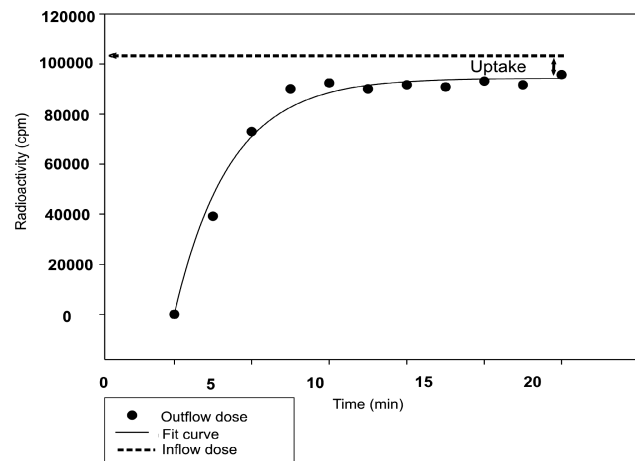


Figure 4. Fitted experimentally obtained dilution profile curve within the inflow period.

### 2.3.3 Endothelium removal procedure

$^{125}\text{I}$ -LDL uptake was evaluated before and after the perfusion with deoxycholic acid. After blood vessel had been prepared as previously described (see section above) Resistance changing device was applied to achieve a constant perfusion pressure ( $60 \pm 10$  mmHg). When the target pressure was achieved, the period of equilibration (15-30 min) was allowed. Then, the deoxycholic acid was continuously injected ( $100 \mu\text{L}/\text{min}$ ) into the blood vessel by using syringe infusion pump (Sage instruments, Inc., USA) for 3 minutes in order to chemically remove the endothelium (21, 22, 23). The final concentration of deoxycholic acid in the perfusion solution was 2.5 mM. After the recovery period (about 15 min) the  $^{125}\text{I}$ -LDL standard solution ( $100 \mu\text{L}/\text{min}$ ) was continuously injected into the blood vessel (inflow dose), by using rapid infusion pump for 10 minutes. Samples were collected and measured as described above.

### 2.3.4 Reagents

The composition of Krebs-Ringer physiological solution contained (in mM): NaCl 117, KCl 4.7,  $\text{NaHCO}_3$  24.8,  $\text{MgSO}_4 \cdot 7\text{H}_2\text{O}$  1.2,  $\text{CaCl}_2$  2.5,  $\text{KH}_2\text{PO}_4$  1.2 and D-glucose 11.1 (Merck, Darmstadt). Evans Blue Dye solution contained 0.33 mg EBD per ml of  $\text{H}_2\text{O}$  distilled.  $^{99\text{m}}\text{Tc}$ -Nanocis is rhenium sulfide nanocolloid (CIS Bio International, France) in which 95% of the particles were between 8 and 68nm, approximately (mean around 23-25nm). This nanocolloid was radio-labeled with technetium ( $^{99\text{m}}\text{Tc}$ ) with a half-life of 6 hours. All experiments were performed in the time frame of 4 hours after preparation of  $^{99\text{m}}\text{Tc}$  rhenium sulphide (Nanocolloid) in which stability of labeled product was maintained.  $^{99\text{m}}\text{Tc}$ -Nanocis was prepared according to the manufacturer's instructions (CIS Bio International, France).  $^{99\text{m}}\text{Tc}$ -Nanocis solution for our experiments

contained 400 MBq  $^{99m}\text{Tc}$  and this colloid was diluted with water for injection until 2 ml.  $^{125}\text{I}$ -Low density lipoprotein (Biomedical Technologies Inc, USA, Catalogue no. BT-903); specific activity: 0.102 $\mu\text{Ci/ml}$ ; quantity: 525  $\mu\text{Ci/2ml}$ .

### 2.3.5 Statistical analysis

Paired t - test with the significance threshold of  $p < 0.05$  was used for statistical comparisons of data between  $U_s$  under different pressures. All statistical calculations were done with the computer program SPSS, version 13.0. Data are presented as mean  $\pm$  standard error (SE).

## RESULTS

### Rapid dual – isotope dilution method

We determined the dilution profiles for  $^{125}\text{I}$ -LDL and  $^{99m}\text{Tc}$ -Nanocis Using Rapid dual–isotope dilution method at the pressure of 10, 80 and 140 mmHg, in the blood vessel segment during one passing (100  $\mu\text{L}$  bolus injection) of the tracers. These profiles showed the logarithmic normal distribution (Eq. 1) and were shifted to the left from the higher to the lower values of the pressure. Our results showed that there was no statistically significant difference between dilution profiles for  $^{99m}\text{Tc}$ -Nanocis and  $^{125}\text{I}$ -LDL, suggesting that the transport of  $^{125}\text{I}$ -LDL could not be precisely determined in this way because it was in the range of the standard error. Also, we measured the accumulation of the  $^{125}\text{I}$ -LDL in each segment. These results showed that at 10 mmHg there was no radioactivity in any segment; at 80 mmHg 0.02% radioactivity of the total injected dose was measured only in the cranial segment and at 140 mmHg 0.05% of the injected dose was measured in the cranial segment, 0.02% in the medial and 0.01% in the cardiac. segment According to these results, the blood vessel wall uptake of  $^{125}\text{I}$ -LDL has very low capacity and is extremely slow. Due to these experimental results, we decided to change the protocol and the continuous 10 minutes perfusion of the  $^{125}\text{I}$ -LDL was applied (steady state method).

### Steady state method

The experimental data were analyzed by using a method described in the previous section and the results are shown in Table 1.

Table 1. Calculated parameters:  $U_s$  and 5T, obtained from experimental data at lower ( $70 \pm 10$  mmHg) and higher ( $140 \pm 10$  mmHg) perfusion pressure.

Pressure (mmHg)	$70 \pm 10$	$140 \pm 10$
Steady state uptake ( $U_s$ %)	Not detectable	$3.52 \pm 1.07$
5T (min)	$3.33 \pm 0.4$	$4 \pm 0.6$

The values are represented as mean  $\pm$  SE (standard error)

When lower pressure was applied ( $70 \pm 10$  mmHg), by increasing intravascular resistance by using resistance changing device at the end of cranial cannula, corresponding  $U_s$  (steady state uptake) of  $^{125}\text{I}$ -LDL was within the value of standard error ( $\pm 1.3$  %) and not detectable. The value of  $b$  coefficient, of the fitted experimental data (Eq 2), which describes the dynamics of  $^{125}\text{I}$ -LDL passage through the blood vessel wall, was  $2.5 \pm 0.08$  and 5T parameter (the time within which the steady state was achieved) was  $3.33 \pm 0.4$  min. Furthermore, our results showed that at the higher perfusion pressure ( $140 \pm 10$  mmHg) calculated  $U_s$  was  $3.52 \pm 1.07$ ,  $b$  coefficient was  $1.25 \pm 0.03$  and 5T was  $4 \pm 0.6$  min. These results are statistically significant when compared to the results obtained at lower pressure ( $p < 0.05$ ).

After sampling, the blood vessel was cut into 3 segments and radioactivity accumulation of the  $^{125}\text{I}$ -LDL in the blood vessel wall was measured in each segment with gamma counter (Wallac Wizard 1400). Our results showed that accumulation of the  $^{125}\text{I}$ -LDL in the blood vessel wall was  $0.06 \pm 0.03$  (% of the inflow dose). Also, our results showed that the most  $^{125}\text{I}$ -LDL radioactivity was in the cranial and the least in the cardiac blood vessel segment (Table 2).

Table 2. Distribution of accumulated  $^{125}\text{I}$ -LDL radioactivity in the different segments of the isolated blood vessel.

Arterial segment	Distribution (%)
Cranial segment	$61.9 \pm 8.7$
Mid segment	$24.6 \pm 5.9$
Cardiac segment	$13.5 \pm 3.1$

The values are represented as mean  $\pm$  SE (standard error)

According to these results, the intact endothelium is a strong barrier for the LDL uptake by the blood vessel wall, allowing only a low accumulation of LDL. It means that under physiological conditions we cannot expect any accumulation of LDL in the blood vessel wall. That is why we decided to remove the endothelium to clarify the influence of endothelium damage on the LDL uptake by the blood vessel wall.

### Endothelium removal

The LDL uptake by the blood vessel wall under Steady state condition was investigated on the isolated blood

vessel segment with the removed endothelium. Endothelium removal procedure was described in the previous section. Our preliminary results suggest that:

- Us was 9.2%;
- accumulation of the LDL in the blood vessel wall was 0.1%;
- in these experiments, unlike in all other (with intact endothelium), we detected significant radioactivity (0.4%) in the medium surrounding the blood vessel in the water bath (external side of the blood vessel). This indicates that LDL passes through the whole blood vessel wall.

## DISCUSSION

Our experimental model could be used to accurately describe LDL uptake by the blood vessel wall during its passage through intravascular space. Until now many studies have tried to explain the transport of LDL through the blood vessel wall and its accumulation in the wall because of its essential role in the development of atherosclerosis (3). All of those studies were performed either on cell mono-layers (4), or on isolated blood vessel strips (13) or segments (11, 14) however without dynamic flow. That was the main reason why we decided to develop a new experimental model in which we used the isolated blood vessel segment with constant perfusion flow because the response obtained in this way is more similar to *in vivo* responses than in previously mentioned experiments (4, 11, 13, 14).

First we used Rapid dual isotope method to research LDL uptake by the blood vessel wall during one passing of the radio-labeled molecules. The results obtained by using this method show that the blood vessel wall uptake of  $^{125}\text{I}$ -LDL has very low capacity and slow dynamics. Due to these experimental results, the protocol has been changed and prolonged (12 minutes) and continual perfusion of  $^{125}\text{I}$ -LDL molecules was applied (Steady state method). The results obtained from the Steady state method indicate very low LDL uptake by the blood vessel wall with intact endothelium which is in accordance with the results of other studies (4, 11, 13, 14, 16).

Also, our results show that at perfusion pressure of  $140 \pm 10$  mmHg the 5T parameter value (the time within which the steady state was achieved) was higher than at  $70 \pm 10$  mmHg, but without significant difference between two 5T parameters ( $p > 0.05$ ). Lack of significant time differences within which the steady state is developed indicate that dynamics of  $^{125}\text{I}$ -LDL passage through the blood vessel wall was similar at applied perfusion pressures ( $70 \pm 10$  mmHg and  $140 \pm 10$  mmHg).

Another advantage of this method is the possibility to describe dynamics of  $^{125}\text{I}$ -LDL uptake by the blood vessel wall during a short period of time (seconds and minutes).

There are no literature data that describe this phenomenon in this way. Up to now arteries have been incubated in the presence of radio-labeled LDL for a longer period of time (5 min, 30 min, 60 min) however without perfusion flow (13, 14).

It has been indicated that hypertension has the impact on arterial disease susceptibility (3, 4, 6-8) and that during hypertension LDL entry into arterial wall is enhanced due to changes of endothelium permeability (9,10). We used different pressures in our method ( $0.70 \pm 10$ ,  $140 \pm 10$  mmHg) in order to investigate whether pressure has any contribution to LDL transport. When lower pressure was applied corresponding Us was not detectable (Table 1) but after applying the higher pressure we obtained the Us of  $3.52 \pm 1.07\%$  which is in accordance with others (4, 10, 11, 14). Furthermore Meyer et al. (11) showed in their study that pressure-induced wall distension unlike the pressure itself is the reason of increased endothelial permeability for macromolecules such as LDL.

According to all of these results the intact endothelium is a strong barrier for the LDL uptake by the blood vessel wall, therefore under physiological conditions with intact endothelium we cannot expect large accumulation of LDL in the blood vessel wall. Cancel et al. (4) indicated that LDL can pass through endothelium mainly through "leaky junctions" (90.9%) as its pathways, which are associated with leaky cells when they are dividing or in the state of turnover, the processes where hypertension has its role (10, 24).

Assuming that intact endothelium is a strong barrier we decided to remove it by using deoxycholic acid. The results obtained after endothelial removal procedure showed that Us of LDL was almost 3 times higher than with intact endothelium (9.2%) ( $p < 0.05$ ), and that accumulation of the LDL in the blood vessel wall was 0.1% (compared to 0.06 % in intact endothelium). These findings are also in accordance with the results of other studies (11, 13).

Finally, we concluded that our experimental model together with the mathematical procedures could be used to describe precisely (with high sensitivity) the LDL uptake by the blood vessel wall during its passage through intravascular space. Further investigations are necessary in order to clarify the mechanisms underlying the LDL uptake and its contribution to better understanding of the development of atherosclerosis and its future prevention.

## ABBREVIATIONS

- Ach – acetylcholine
- cpm - counts per minute
- EBD - Evans blue dye
- KRS - Krebs-Ringer physiological solution

LDL - low-density lipoprotein

SE - standard error

Us - steady state uptake

### ACKNOWLEDGMENTS

This work was supported by the Ministry of Science in Serbia, Grant III41007.

### REFERENCES

- Hoff HF, Heideman CL, Jackson RL, Bayardo RJ, Kim HS, Gotto AMJ. Localization patterns of plasma apolipoproteins in human atherosclerotic lesions. *Circ Res* 1975; 37: 72–9.
- Ross R. Atherosclerosis: a defense mechanism gone awry. *Am J Pathol* 1993; 143: 987–1002.
- Sun N, Wood NB, Hughes AD, Thom SA, Xu XY. Effects of transmural pressure and wall shear stress on LDL accumulation in the arterial wall: a numerical study using a multilayered model. *Am J Physiol Heart Circ Physiol* 2007; 292: H3148–57.
- Cancel L, Fitting A, Tarbell JM. In vitro study of LDL transport under pressurized (convective) conditions. *Am J Physiol Heart Circ Physiol* 2007; 293: H126–32.
- Nielson LB. Transfer of low-density lipoprotein into the arterial wall and risk of atherosclerosis. *Atherosclerosis* 1996; 123: 1–15.
- Olgac U, Kurtcuoglu V, Poulikakos D. Computational modeling of coupled blood-wall mass transport of LDL: effects of local wall shear stress. *Am J Physiol Heart Circ Physiol* 2008; 294: H909–19.
- Tarbell JM. Mass transport in arteries and the localization of atherosclerosis. *Annu Rev Biomed Eng* 2003; 5: 79–118.
- Yang N, Vafai K. Modeling of low-density lipoprotein (LDL) transport in the artery— effects of hypertension. *Int J Heat Mass Transf* 2006; 49: 850–67.
- Bretherton KN, Day AJ, Skinner SL. Effect of hypertension on the entry of I-labeled low density lipoprotein into the aortic intima in normal-fed rabbits. *Atherosclerosis* 1976; 25: 99–106.
- Wu CH, Chi JC, Jerng JS, et al. Transendothelial macromolecular transport in the aorta of spontaneously hypertensive rats. *Hypertension* 1990; 16: 154–61.
- Meyer G, Merval R, Tedgui A. Effects of pressure-induced stretch and convection on low-density lipoprotein and albumin uptake in the rabbit aortic wall. *Circ Res* 1996; 79: 532–40.
- Cheng C, Tempel D, van Haperen R, et al. Atherosclerotic lesion size and vulnerability are determined by patterns of fluid shear stress. *Circulation* 2006; 113: 2744–53.
- Fry DL, Haupt MW, Pap JM. Effect of endothelial integrity, transmural pressure, and time on the intimal-medial uptake of serum 125I-albumin and 125I-LDL in an in vitro porcine arterial organ-support system. *Arterioscler Thromb Vasc Biol* 1992; 12: 1313–28.
- Curmi PA, Juan L, Tedgui A. Effect of transmural pressure on low density lipoprotein and albumin transport and distribution across the intact arterial wall. *Circ Res* 1990; 66: 1692–702.
- Prosi M, Zunino P, Perktold K, Quarteroni A. Mathematical and numerical models for transfer of low-density lipoproteins through the arterial walls: a new methodology for the model set up with applications to the study of disturbed luminal flow. *J Biomech* 2005; 38: 903–17.
- Dabagh M, Jalali P, Tarbell JM. The transport of LDL across the deformable arterial wall: the effect of endothelial cell turnover and intimal deformation under hypertension. *Am J Physiol Heart Circ Physiol* 2009; 297: H983–96.
- Tronc F, Wassef M, Esposito B, Henrion D, Glagov S, Tedgui A. Role of NO in flow-induced remodeling of the rabbit common carotid artery. *Arterioscler Thromb Vasc Biol* 1996; 16: 1256–62.
- Rosic M, Pantovic S, Lucic A, Ribarac-Stepic N, Andjelkovic I. Kinetics of thyroxine (T4) and triiodothyronine (T3) transport in the isolated rat heart. *Exp Physiol* 2001; 86: 13–8.
- Kostic MM, Rosic GL, Segal MB, Rosic MA. Biphasic L-arginine uptake by the isolated guinea-pig heart. *Exp Physiol* 1995; 80: 969–79.
- Rosic M, Pantovic S, Rankovic V, Obradovic Z, Filipovic N, Kojic M. Evaluation of dynamic response and biomechanical properties of isolated blood vessel. *J Biochem Biophys Methods* 2008; 70: 966–72.
- Rocha AP, Carvalho LC, Sousa MA, et al. Endothelium-dependent vasodilator effect of Euterpe oleracea Mart (Açai) extracts in mesenteric vascular bed of the rat. *Vascul Pharmacol* 2007; 46: 97–104.
- Soares de Moura R, Resende AC, Emiliano AF, et al. The role of bradykinin, AT2 and angiotensin II on the isolated mesenteric vascular bed of the rat. *Br J Pharmacol* 2004; 141: 860–6.
- Ralevic V. The involvement of smooth muscle P2X receptors in the prolonged vasorelaxation response to purine nucleotides in the rat mesenteric arterial bed. *Br J Pharmacol* 2002; 135: 1988–94.
- Lin SJ, Jan KM, Chien S. Role of dying endothelial cells in transendothelial macromolecular transport. *Arteriosclerosis* 1990; 10: 703–9.